The Mechanochemical Synthesis of Magnesium Hydride Nanoparticles

Drew A. Sheppard*, Mark Paskevicius, Craig E. Buckley

Department of Imaging and Applied Physics at Curtin University of Technology, GPO Box U 1987, Perth 6845, Australia.

Abstract

A mechanochemical method was used to synthesise magnesium hydride nanoparticles with an average crystallite size of 6.7 nm. The use of a reaction buffer was employed as a means of particle size control by restricting agglomeration. Increasing the amount of reaction buffer resulted in a decrease in crystallite size, as determined via x-ray diffraction, and a decrease in particle size, evidenced by Transmission Electron Microscopy.

*Corresponding Author

Drew A. Sheppard

Department of Imaging and Applied Physics at Curtin University of Technology, GPO Box U 1987, Perth 6845, Australia.

Email: drew.sheppard@gmail.com

Phone: 61 8 92664955

Fax: 61 8 92662377

1. Introduction

Hydrogen is an ideal energy carrier and contains more chemical energy per weight than any hydrocarbon. It can be used in a fuel cell to produce water as the only emission. However, the effective storage of hydrogen still remains a barrier to the implementation of a hydrogen economy. Magnesium has been widely studied due to its ability to absorb 7.7 wt.% of hydrogen but its use is impeded by a high thermal stability and poor sorption kinetics. The kinetic issue has largely been overcome by introducing catalytic metal oxides via ball-milling [1, 2]. Recently, theoretical work has suggested that reducing the MgH_2 particle size below 10 nm [3] should alter the thermodynamics of MgH_2 with the effect becoming appreciable below 3 nm [3 - 6]. Traditional ball milling can reduce MgH_2 crystallite sizes to ~7 nm [2] but these consist of crystallite domains within much larger particles. Subsequent heating to 300°C to release hydrogen also results in substantial crystallite growth [2, 7]. Recent efforts to produce nanometre sized magnesium include magnesium melt infiltration into porous carbon [8] and sonoelectrochemical deposition from magnesium salt solutions [9].

Mechanochemical synthesis is a technique that employs solid state displacement reactions during ball milling [10]. This method has been used recently to synthesize AlH_3 [11] and $Mg(AlH_4)_2$ [12]. However, these authors did not use particle size control methods, such as varying: the amount of buffering agent; the milling time; the milling collision energy and; milling temperature, that have previously been used to produce separated, nanosized particles of oxides [13], metals [14, 15] and sulphides [16]. Employing the particle size control methods can produce particles as small as 4 nm [17] embedded in larger by-product phase particles. Herein, for the first time, we present the results of the synthesis of MgH_2 nanoparticles using the mechanochemical method. In addition, the variation in the microstructure of the synthesised MgH_2 was examined as a function of the quantity of LiCl used as a reaction buffer. The synthesis of MgH_2 was achieved by utilising the following chemical reaction:

$$2LiH + MgCl_2 \rightarrow MgH_2 + 2LiCl \qquad (1)$$
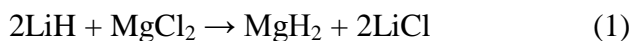
2. Experimental

All handling of chemicals and sealable milling vials was undertaken in an argon-atmosphere glovebox in order to minimise oxygen (O_2 < 1 ppm) and water (H_2O < 1 ppm) contamination. LiH (Sigma-Aldrich, 95%), $MgCl_2$ (Sigma, $\geq$ 98%) and LiCl (Sigma-Aldrich, $\geq$ 99.9%) were used as starting reagents without further purification. All reagents were ball milled separately for 3 hours at a ball-to-powder ratio of 30:1 prior to use, as reducing the grain size of the starting reagents has been shown to accelerate the kinetics of mechanochemical reactions [16]. Four samples of MgH_2 were produced using various amounts of LiCl buffer added to the starting reagents. The amount of LiCl added for each sample corresponded to 0 (sample MgH_2-A), 1.05 (sample MgH_2-B), 2.62 (sample MgH_2-C) and 6.82 (sample MgH_2-D) moles of LiCl added to the left hand side of Equation 1. X-ray diffraction patterns (XRD) were collected from samples sealed in 0.5 mm glass capillaries at the Australian Synchrotron using a wavelength of 0.1 nm (12.4 keV) for 900 seconds each. Rietveld analysis of the XRD patterns was performed using the software package TOPAS (Bruker AXS, Karlsruhe, Germany). The crystallite sizes were determined from an LVol-IB method (volume averaged column height calculated from the integral breadth) which provides a good measure of the volume-weighted mean crystallite size [18].

3. Results and discussion

Figure 1 displays the XRD patterns for MgH_2-A, MgH_2-B, MgH_2-C and MgH_2-D. After 18 hours of milling (ball to powder ratio of 90:1), XRD of MgH_2-A reveals only MgH_2 and LiCl (Figure 1A). No starting reagents are detectable. As expected, the MgH_2 peak intensities decrease for subsequent samples as the amount of LiCl added to the initial starting reagents increases. The XRD patterns for MgH_2-A, MgH_2-B and MgH_2-C (Figure 1A, 1B and 1C) show a minor unknown peak at d = 0.3142 nm which is expected to be a minor reagent impurity phase that was not detected by laboratory based XRD. A peak at d = 0.2075 nm clearly discernable in MgH_2-D is attributed to 316 stainless steel, a minor contaminant from the ball milling canister (also not detected in laboratory based XRD). From Rietveld refinement the MgH_2 crystallite sizes for MgH_2-

A, MgH$_2$-B, MgH$_2$-C and MgH$_2$-D were determined to be 10.1 ± 0.3 nm, 7.6 ± 0.3 nm, 6.7 ± 0.4 nm and 6.7 ± 0.7 nm respectively.

Though synchrotron XRD was able to distinguish MgH$_2$ in the sample MgH2-D, it was not detected by laboratory based XRD. As a result of the inability to detect minor light element phases, quantitative phase analysis from XRD diffraction may prove unreliable in measuring the extent to which the reaction in Equation 1 is complete. Consequently, hydrogen sorption measurements were performed to determine the MgH$_2$ content in each sample. The samples were placed in a manometric hydrogen sorption apparatus, without exposure to air, and out-gassed at 300°C for 24 hours. This temperature is insufficient to remove hydrogen from any unreacted LiH and therefore the subsequent hydrogen absorption can be attributed solely to Mg. In considering the extent to which the reaction in Equation 1 had gone to completion during ball milling for each sample, the fact that the starting reagent, LiH, had only 95% purity must be considered. From the hydrogen sorption measurements it was found that for MgH$_2$-A, MgH$_2$-B, MgH$_2$-C and MgH$_2$-D the reaction was 94.5, 84.9, 82.2 and 78.1 % complete, respectively. The decrease in the extent to which Equation 1 is complete is an expected consequence of the dilution of the starting reagents, LiH and MgCl$_2$, which hinders reagent contact and thus reaction kinetics.

Representative Transmission Electron Microscopy (TEM) images for each sample are displayed in Figure 2. MgH$_2$-A (Figure 2A) primarily showed large geometrical shapes (typically hexagons) 1 to 2 μm in size. The large geometrical structures, which were initially dark, showed a steadily increasing light band over time (indicated by an arrow in Figure 2A) around the outer edge on exposure to the electron beam. This effect ceased after some minutes. The growth of the light band suggested that these micron sized particles are MgH$_2$ that underwent hydrogen desorption under the beam. MgH$_2$-B showed no large geometrical shapes such as those in MgH$_2$-A. Typical morphologies (Figure 2B) consisted of agglomerations of irregularly shaped particles 15 - 40 nm in size. Time lapse TEM images showed that some particles within the agglomerates (indicated by arrows in Figure 2B) changed under the electron beam over the course of several minutes. MgH$_2$-C comprises of only a single morphology consisting of well

dispersed 12 – 20 nm particles. Given the average MgH_2 crystallite from XRD is 6.7 nm, it is suggested that each particle in MgH_2-C consists of several crystallite domains. MgH_2-D is largely homogenous and doesn't show any readily recognisable particle morphology. High magnification TEM identified lattice fringing regions that extended for 2 – 4 nm. The lattice fringing was limited to the MgH_2 *hkl* = 020 plane suggesting very small MgH_2 crystallites were synthesised. Whether these crystallites were part of larger grains or individually dispersed was difficult to determine. However it should be noted that the crystallite sizes, as seen by lattice fringing, in sample MgH_2-D are comparable to that determined via XRD. This is in contrast to other recent efforts in producing nanometre scale magnesium [9] in which the crystallite size, as determined via TEM, is almost an order of magnitude smaller than that determined via XRD. Such a difference may be attributed to the fact that TEM samples therein may not be representative of the average sample structure in comparison to XRD.

An electrochemical method has also recently been used to synthesise a colloid containing 18 mass % 5 nm Mg nanoparticles [19] stabilised by tetrabutylammonium bromide (TBA). After hydriding, the material displayed a hydrogen desorption pressure of 0.3 kPa at just 85°C. The desorption pressure at this temperature is significantly higher than that predicted by theoretical calculations for even 1 nm MgH_2 particles [3]. It is in our opinion that such a measured desorption pressure is not a result of the particle size, as claimed by the authors, but by a chemical interaction between the Mg and the ammonium salt causing a destabilisation of the hydride phase. Such large changes in the thermodynamics of hydrides have previously been observed for AlH_3-adduct systems [20]. The absence of a TBA melting event in Differential Thermal Analysis [19], which usually occurs at ~100°C, further suggests that a chemical interaction between the Mg surface and TBA is responsible for the altered thermodynamics observed for the hydrogen desorption over TBA stabilised Mg nanoparticles.

4. Conclusions

In the present work the mechanochemical synthesis of MgH_2 has been undertaken with varying LiCl buffer amounts. Increasing buffer results in MgH_2 crystallite sizes down to 6.7 nm, measured via XRD, whilst TEM investigations show that increasing buffer results in smaller, more highly dispersed MgH_2 nanoparticles. The size of these MgH_2 particles approaches theoretical predictions for thermodynamic changes and the MgH_2 is only physically bound by the LiCl. Removal of the LiCl salt by-product phase has thus far proved difficult due to either the high reactivity or the solubility of MgH_2 in solvents which will dissolve LiCl. Preliminary hydrogen sorption measurements also indicate that an increase in the hydrogen equilibrium pressure occurs for samples with higher LiCl buffers (and hence smaller particle sizes). The removal of the by-product phase and thermodynamic measurements are the subject of a forthcoming publication.

Acknowledgements

References

[1] G. Barkordarian, T. Klassen, R. Bormann, J. Alloys Compd. 364 (2004) 242-246.

[2] K.F. Aguey-Zinsou, J.R. Ares Fernandez, T. Klassen, R. Bormann, Mater. Res. Bull. 41 (2006) 1118-1126.

[3] K.C. Kim, B. Dai, K.J. Johnson, D.S. Sholl, Nanotechnol. 20 (2009) 204001.

[4] J.J. Liang, Appl. Phys. A 80 (2005) 173-178.

[5] R.W.P. Wagemans, J.H. van Lenthe, P.E. de Jongh, A.J. van Dillen, K.P. de Jong, J. Am. Chem. Soc. 127 (2005) 16675-16680.

[6] S. Cheung, W.Q. Deng, A.C.T. van Duin, W.A. Goddard, J. Phys. Chem. A 109 (2005) 851-859.

[7] J. Huot, J.F. Pelletier, L.B. Lurio, M. Sutton, R. Schulz, J. Alloys Compd. 348 (2003) 319-324.

[8] P.E. de Jongh, R.W.P. Wagemans, T.M. Eggenhuisen, B.S. Dauvillier, P.B. Radstake, J.D. Meeldijk, J.W. Geus, K.P. de Jong, Chem. Mater. 19 (2007) 6052-6057.

[9] I. Haas, A. Gedanken, Chem. Comm. (2008) 1795-1797.

[10] J. Ding, W.F. Miao, P.G. McCormick, R. Street, Appl. Phys. Lett. 67 (1995) 3804-3806.

[11] H.W. Brinks, A. Istad-Lem, B.C. Hauback, J. Phys. Chem. B 110 (2006) 25833-25837.

[12] R.A. Varin, C. Chiu, T. Czujko, Z. Wronski, J. Alloys Compd. 439 (2007) 302-311.

[13] J. Ding, T. Tsuzuki, P.G. McCormick, Nanostruct. Mater. 8 (1997) 75-81.

[14] C. Suryanarayana, Prog. Mater. Sci. 46 (2001) 1-184.

[15] M. Paskevicius, J. Webb, M.P. Pitt, T.P. Blach, B.C. Hauback, E.MacA. Gray, C.E. Buckley, J Alloys Compd. 481 (2009) 595-599.

[16] T. Tsuzuki, J. Ding, P.G. McCormick, Physica B 239 (1997) 378-387.

[17] P.G. McCormick, T. Tsuzuki, J.S. Robinson, J. Ding, Adv. Mater. 13 (2001) 1008-1010.

[18] A.A. Coelho, Topas User Manual, Bruker AXS GmbH, Karlsruhe, Germany, 2003.

[19] K.F. Aguey-Zinsou, J.R. Ares-Fernandez, Chem. Mater. 20 (2008) 376-378.

[20] J. Graetz, Chem. Soc. Rev. 38 (2009) 73-82.

Figures

Figure 1: Synchrotron X-ray diffraction data on sample (A) MgH_2-A, (B) MgH_2-B, (C) MgH_2-C and (D) MgH_2-D. 316 SS refers to stainless steel type 316.
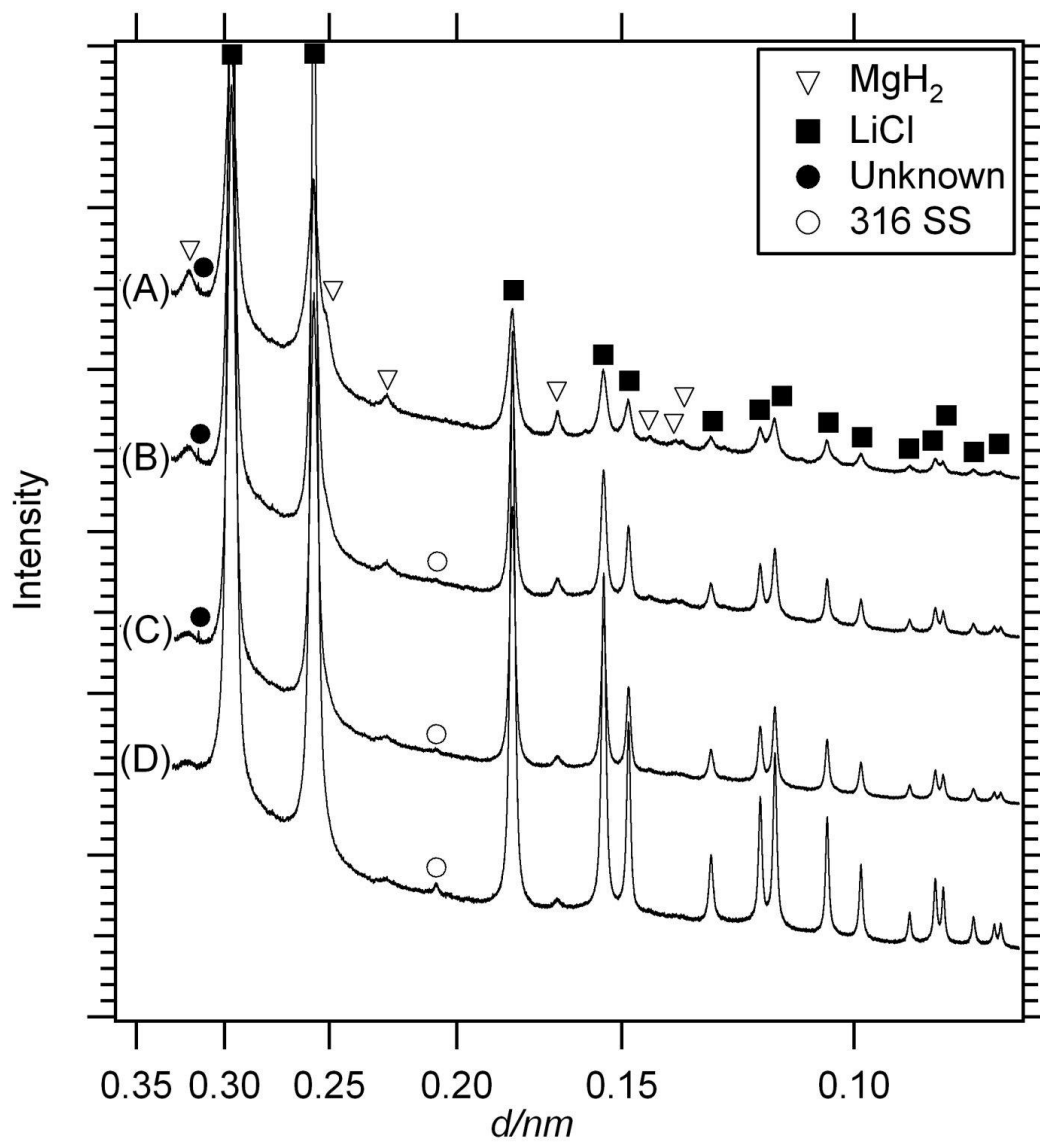
Figure 2: Representative transmission electron microscopy images of (A) MgH$_2$-A, (B) MgH$_2$-B, (C) MgH$_2$-C and (D) MgH$_2$-D. White arrows indicating regions that underwent decomposition during exposure to the electron beam.